Scientific paper

Impedance of Electrochemically Modified Graphite

Katja Magdić, Krešimir Kvastek and Višnja Horvat-Radošević*

DMER, Ruđer Bošković Institute, Bijenička c. 54, 10000 Zagreb, Croatia

** Corresponding author: E-mail: vhorvat@irb.hr*

Received: 05-02-2014

Paper based on a presentation at the 4th RSE-SEE 2013 Symposium on Electrochemistry in Ljubljana, Slovenia

Abstract

Electrochemical impedance spectroscopy, EIS, has been applied for characterization of electrochemically modified graphite electrodes in the sulphuric acid solution. Graphite modifications were performed by potential cyclization between potentials of graphite oxide formation/reduction, different number of cycles, and prolonged reduction steps after cyclization. Impedance spectra measured at two potential points within double-layer region of graphite have been successfully modeled using the concept of porous electrodes involving two different electrolyte diffusion paths, indicating existence of two classes of pores. The evaluated impedance parameter values show continuous changes with stages of graphite modification, indicating continuous structural changes of pores by number of potential cycles applied. Differences of impedance parameter values at two potential values indicate the potential induced changes of solution properties within the pores of modified graphite.

Keywords: Graphite, oxidized graphite, expanded graphite, electrochemical impedance spectroscopy

1. Introduction

Carbon allotrope, graphite, is a crystalline and layered compound, with carbon atoms covalently bonded into a hexagonally structured basal planes in each layer.[1,2] Whereas size and orientation of graphitic crystallites define texture, porosity and electrical conductivity of graphite material, the layers bonded by weak forces, make graphite matrix extremly prone to intercalation of ions or molecules from electrolyte. Under anodic polarization conditions, intercalation in combination with formation of different oxygenated groups, results in formation of expanded and even exfoliated graphite oxide.[3–6] Generally, any expanded form of graphite oxide can be reduced to expanded graphite that becomes a material of numerous potential applications in different areas, including batteries and supercapacitors.[2,6,7] A special case is reduced form of exfoliated graphite oxide that has been found important for production of actually engaging graphene sheets,[8–10] having unique physical and chemical properties.[11,12]

Electrochemical properties of complex interfacial electrode/electrolyte region formed at the contact of graphite/graphene and an electrolyte has usually been explored by various electrochemical methods, including electrochemical impedance spectroscopy, EIS.[2,7,11,13–18] The principal advantage of EIS over other techniques is possibility to separate different steps and stages taking part during interfacial reaction(s) in a complex system, and/or to follow current density distribution as an effect of electrode geometry.[19,20]

Fresh graphite electrode has usually been investigated within the frame of battery investigations and so in conditions of a charge transfer reaction, including intercalation, or some redox probe reaction. For such a purpose, graphite is prepared as a powder forming active mass of certain thickness attached to some substrate, exposing rough and/or porous surface toward an electrolyte. Roughness and/or porosity of graphite electrode surface has nominally been accounted for by the *so called* constant phase element, CPE, as the non-faradaic, *i.e*. double-layer related impedance part.[13–16] General theoretical justification for capacitive dispersion, commonly observed at all solid electrodes, is based on distribution of time constants related to locally distributed electrode surface irregularities,[21] or to the effects of specific adsorption of electrolyte ions.[16,22] The same kind of double-layer impedance modeling has widely been accepted and announced also for exfoliated graphite sheets[23] and reduced forms of graphite and graphene oxides,[17,24] respectively. For double-layer impedance of pressed microstructured graphite at potentials of not any faradaic reaction, however, the *so called* distributed constant-phase, or transmission line element, TL, was applied,[25] following already developed im-

pedance function for porous electrodes.[26] TL should also account for non-uniform current distribution, but in difference to CPE, differently within different frequency ranges.[19]

Modeling of double-layer impedance in absence of faradaic reaction(s) is especially important for electrochemical capacitor investigations, where high specific capacitance values and fast access of ions toward electrode surface are of crucial interest.[1,2,6,11,12,27] For such a purpose, graphite has commonly been oxidized and subsequently reduced, what resulted in expansion of graphite host and consequently increased surface area. By this procedure, a surface area based capacitance is additionally increased by a pseudocapacitance induced by fast redox reaction of residual oxygenated surface groups formed by oxidation.[2,6,7] Contrary to nanoporous diamond,[27] activated carbon[28] or glassy carbon[29,30] cases, impedance modeling of graphite/graphene in double-layer potential region is unexpectedly scarce in the literature. In this connection, the papers on some experimental evidence of different impedance spectra measured for graphite oxide and reduced graphite oxide,[7] or decrease of capacitive impedance in going from graphite oxide, *via* graphene oxide to electrochemically reduced graphene oxide should be mentioned,[18] but detailed impedance analysis remains unreached. Therefore, in the present study, electrochemically modifed graphite electrodes in double-layer potential region and sulphuric acid solution are examined using EIS. The results are expected to have an impact for better understanding of graphite properties what could be utilized for various applications.

2. Experimental

All experiments were performed at room temperature in a three-electrode cell, with high surface Pt-spiral counter electrode and Luggin capillary ended Hg/Hg_2SO_4 (sat. K_2SO_4), MSE, electrode (+0.40 V *vs*. saturated calomel electrode, SCE). The working electrode was a 3 mm diameter graphite rod (Goodfellow, UK) sealed into the glass tube, exposing a disc of 0.07 cm^2 of geometric area toward 0.5 mol dm^{-3} H_2SO_4 (high purity BDH, Aristar) electrolyte solution. Graphite electrode was modified electrochemically by 10, 30, 50 and 70 potential cycles applied at the scan rate of 10 mV s^{-1} between –0.70 and 1.60 V. In such a way, modified graphite, denoted as G-M1 to G-M4 electrodes, are formed. Note that in contrast to the potentiostatic anodization procedure, potential cyclization procedure hinders formation of highly exfoliated graphite oxide, and formed un-exfoliated oxide can easily be reduced back to the expanded graphite form.[6] Also, the upper vertex potential value of 1.60 V *vs*. MSE was chosen on the basis of preliminary investigations that showed significant damage of graphite for higher anodic vertex potential values.

After electrochemical modification has been finished, G-M1 to G-M4 graphite electrodes were held at –0.60 V *vs*. MSE for 30 minutes and then tested in fresh, 0.5 mol dm^{-3} H_2SO_4, electrolyte by applying four cycles of CV experiments at 50 mV s^{-1}. Solartron 1287 ECI under *Z*corr software control was used for electrochemical modification and testing CVs. In the set of parallel experiments, graphite electrodes were taken from the cell, dried and held in vacuum conditions prior being scanned by scanning electron microscope (JSM-700F, JEOL, Japan).

EIS was carried out using Solartron equipment (1255B frequency response analyzer and 1287 electrochemical interface) and 10 mV amplitude signal. Frequency, *f*, ranged between 100 kHz and 0.01 Hz with 10 impedance points measured per decade. In an order to attain stationary values, the rest time before each impedance spectrum measurement was always held for at least 10 minutes. Impedance data fittings were performed using Z_{View} software and complex non-linear least square, CNLS, routine with presumed electrical equivalent circuit(s). The models were regressed to experimental data with impedance modulus proportional weighting. Corrections for a three-electrode cell induced artefact impedances present at the highest frequencies[31] were performed according to the procedure described previously.[32] Reasonable fits were defined for small weighted sum of errors of the overall fits, S (≤ 0.1) and standard deviation of each parameter ≤10%. S is defined as:[19]

$$S = \sum_{k=1}^{N} w_k ((Z'_{k(\exp)} - Z'_{k(cal)})^2 + (Z''_{k(\exp)} - Z''_{k(cal)})^2) \quad (1)$$

According to definition of impedance, *Z*, as a complex number, Z_k' and Z_k'' in eqn. (1) are real and imaginary parts of impedance at a frequency $\omega_k = 2\pi f_k$. N is total number of measured frequencies, while *exp* and *calc* denote experimentally measured and calculated impedances, respectively.

3. Results and Discussion

3. 1. Cyclic Voltammetry and SEM Examinations of Graphite Electrodes

Electrochemical oxidation voltammograms of graphite in 0.5 mol dm^{-3} H_2SO_4 performed between 0.70 and 1.60 V *vs*. MSE with 10–70 potential cycles are shown in Figure 1a.

Fig. 1a shows similar CVs for each stage of graphite modification. In positive going scans for each graphite electrode, almost constant current density was measured up to about 0.8 V *vs*. MSE, where moderate increase followed by a sharp increase near anodic vertex potential value is observed. In reverse going scans, almost featureless curves are measured down to –0.5 V *vs*. MSE, where peaks are formed

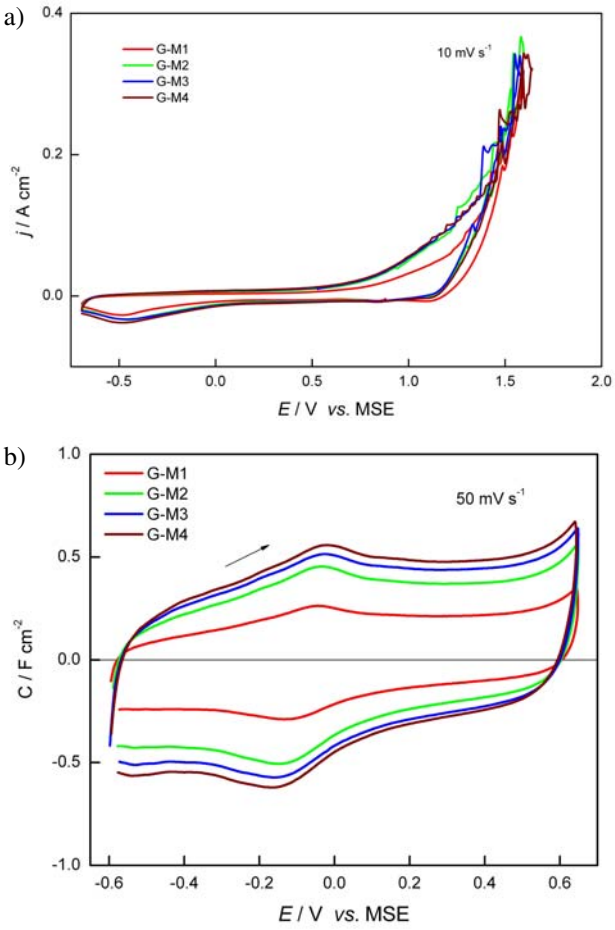

Fig. 1. CVs of graphite electrodes in 0.5 mol dm^{-3} H_2SO_4: (a) The last cycles of graphite modification CVs forming G-M1 to G-M4 electrodes at 10 mV s^{-1} and 10–70 potential cycles; (b) Specific capacitance-potential curves (4^{th} cycles) of G-M1 to G-M4 electrodes measured in double-layer potential region at 50 mV s^{-1}.

for all electrodes. All current density values are generally higher for higher extent of graphite modification attained by higher number of potential scans applied. Increased anodic current density values at about 0.8 V *vs*. MSE, seen for all graphite electrodes, indicate possible insertion of HSO_4- ions that penetrate readily into graphite host matrix.[3,4,14] It has already been pointed out that the onset potential for HSO_4- intercalation ranges between 0.5 to 1.1 V *vs*. MSE and decreases with concentration of sulphuric acid.[3] Electrochemical intercalation is generally considered as a reversible faradaic reaction, proceeding through insertion stage and formation of intercalated compound phase.[4,14] Therefore, lack of de-insertion step in Fig. 1a at about 0.8 V *vs*. MSE is a probable result of low concentration of H_2SO_4 used in present experiments causing low stages of intercalation and lack of phase transition, at least.[4] For all graphite electrodes, rather irreversible reactions of graphite oxide formation, graphite corrosion and oxygen evolution are superimposed to intercalation of HSO_4^- ions[4,14] and seen in Fig. 1a as highly increased current values near the vertex potential of 1.6 V, and reduction peaks at –0.50 V *vs.* MSE. Gradual increase of current densities for graphite electrodes formed by increased number of potential cycles, are probably due to gradually increased surface area caused by graphite surface corrosion induced roughening and expansion of oxidized graphite regions.[9,33] Some extent of surface damage is observed for graphite oxidized by the highest number of potential cycles, G-M4, electrode. Damage of graphite surface should be connected with corrosion of carbon surface promoted by CO_2 evolution at high anodic potentials,[33] or longer time spent at high potentials, where acid penetration can create significant structural defects within graphite layers and failure of material.[5] Figure 1b shows specific capacitance curves of modified graphite electrodes, after electrochemical reduction performed at 0.60 V *vs.* MSE during 30 minutes in 0.5 mol dm3 H_2SO_4 prior measurements. Capacitance values are evaluated from ordinary CVs measured between –0.60 and 0.65 V *vs*. MSE, *i.e.* within double-layer capacitance potential region. Fig. 1b shows higher capacitances for graphite modified by increased number of potential cycles and well shaped peaks formed between –0.10 and –0.20 V *vs*. MSE for all electrodes. As for other carbon electrodes, these peaks should be related to redox reactions of (some between) oxygenated surface groups formed during oxidation.[1,2]

SEM images of all electrochemically modified graphite electrodes show quite similar features and a representative is shown in Figure 2.

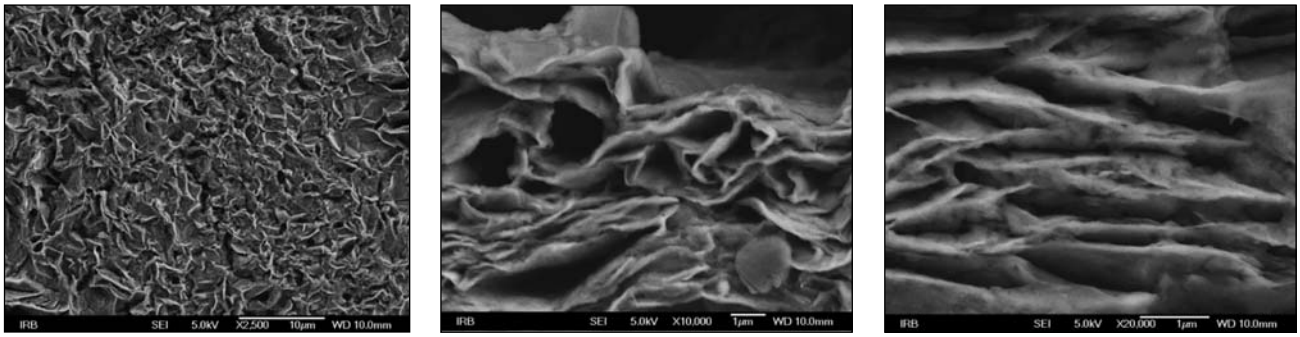

Fig. 2. Representative SEM images (increased magnifications) of graphite modified in 0.5 mol dm^{-3} H_2SO_4 according to Fig.1a.

It appears from Fig. 2 that electrochemically modified graphite surface shows generally a rough structure, while higher magnifications show clearly a layered structure of expanded graphite with few tens of nm thick horizontally oriented planes, where electrolyte can penetrate more deeply. Similar SEMs, showing layered graphite structures, have already been reported for a sulfuric acid intercalated graphite oxide and oxidized/reduced graphite electrodes.[6,9,10] Although images in Fig. 2 show apparently low degree of graphite exfoliation, the remaining stacking of graphite could be disordered. This could also be a reason why materials from the graphite oxidized by the highest number of cycles (70) are dispersed into solution.

3. 2. Experimental Impedance Spectra of Graphite Electrodes

According to definition of impedance as a complex number, $Z(i\omega) = Z' - iZ''$,[19,20] Figure 3 presents Nyquist plots (Z'' *vs.* Z') of electrochemically modified graphite electrodes in 0.5 mol dm^{-3} H_2SO_4, held at –0.20 V *vs.* MSE (near peak potential of Fig. 1b).

By inclined and near –90° sloping lines, impedance spectra in Fig. 3a show almost capacitive responses for all electrochemically modified graphite electrodes, differing only in impedance magnitudes. For the less modified, GM-1 electrode, however, certain bending of impedance line can also be denoted in Fig. 3a. Except significant decrease of impedance magnitudes observed for graphite electrodes modified with higher number of cycles, Fig. 3b shows an apparent lowering of slopes toward –45° above 10 Hz, and also some shifts of all curves toward higher Z' values.

According to definition of impedance as a vector with magnitude $|Z|$ and phase angle $-\varphi$,[19,20] Figure 4 shows impedance spectra of electrochemically modified graphite electrodes in the form of Bode plots, log $|Z|$ and $-\varphi$ *vs.* log ω.

In difference to Nyquist plots that show only low frequency parts of capacitive impedance responses (*cf.* Fig. 3a), Bode plots allow comparison of impedance spectra at all measured frequencies. For all electrochemically modified graphite electrodes, Bode magnitude plots show almost resistive response-related plateaus at broad range of higher frequencies (10^5–10^2 Hz). Below 100 Hz, the slopes are changed toward near –1 sloping curves, characterizing almost capacitive electrode responses. Not ideal capacitive responses for all graphite electrodes are, however, indicated by phase angles lower than –90° at low frequency parts of φ *vs.* log ω dependences in Fig. 4. For the less modified, G-M1 electrode, a continuous decrease of $-\varphi$ values can also be noted at few lowest frequencies. Generally, impedance spectra in Fig. 4 show that continu-

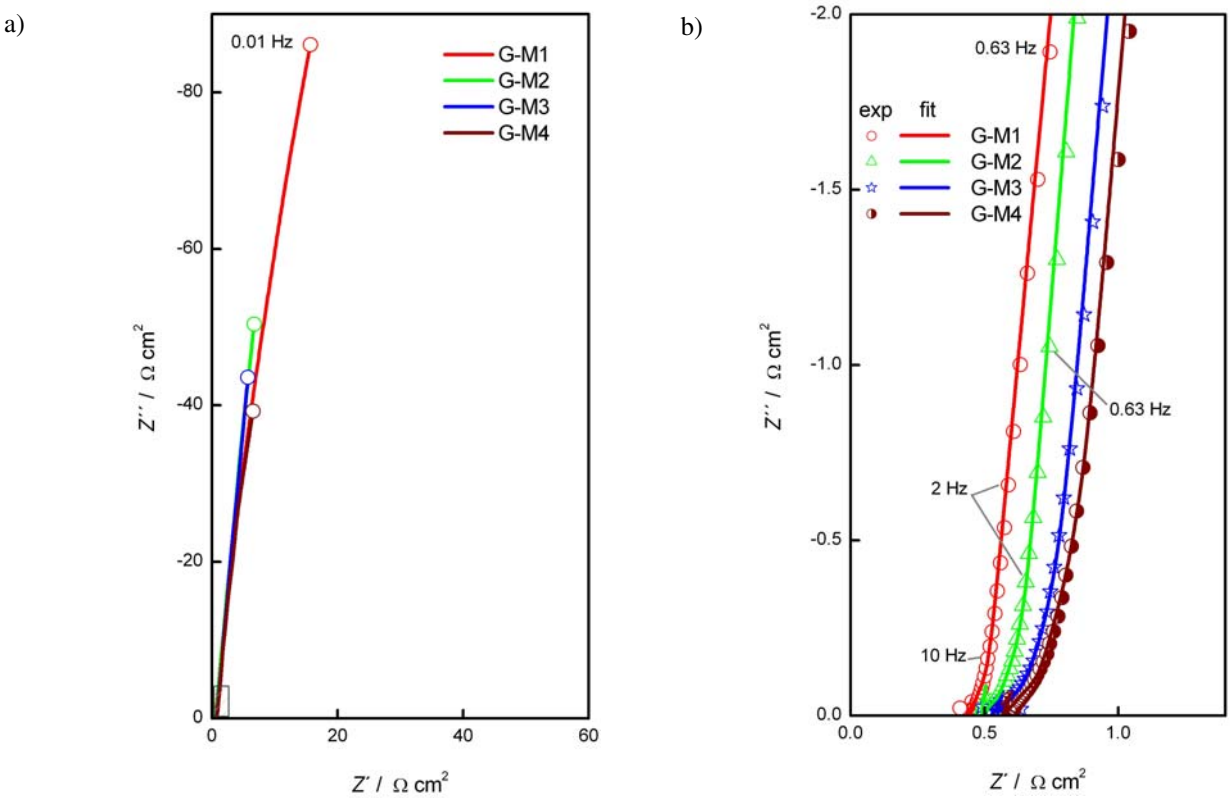

Fig. 3. Nyquist plots (Z'' *vs.* Z') of electrochemically modified graphite electrodes in 0.5 mol dm^{-3} H_2SO_4, measured at –0.20 V *vs.* MSE and presented at: (a) all frequencies; (b) higher frequency region.

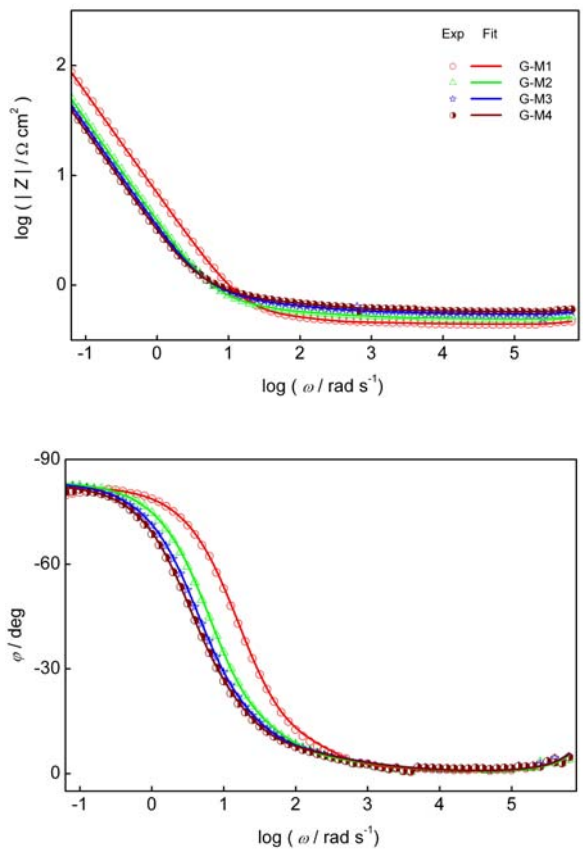

Fig. 4. Bode plots (log| *Z*| and φ *vs.* log ω) of electrochemically modified graphite electrodes in 0.5 mol dm^{-3} H_2SO_4 measured at –0.20 V *vs*. MSE.

ously higher resistive impedances at higher frequencies and continuously lower capacitive impedances at lower frequencies are measured for graphite electrodes modified with higher number of potential cycles.

Figure 5 shows impedance spectra of modified graphite electrodes presented in the form of complex capacitance dispersion, (*C´´vs. C´*), defined on the basis of conversion of capacitive impedance to its reciprocal, admittance, *Y*, according to:[19,22]

$$Y(i\omega) = [Z(i\omega)]^{-1} = (i\omega)(C' - iC'') \quad (2)$$

Generally, the complex capacitance presentation allows clear presentation of dissipative processes for otherwise capacitive electrode responses.[19,22,27] According to eqn. (2), capacitance value is determined by intersection of the real part with *C´* axis at low frequencies, while dissipation is noticed through a contribution of imaginary part, respectively. Fig. 5a shows circle path-behaviour for all electrochemically modified graphite electrodes, what is a general feature of dissipative capacitive electrode response. Diameters of circles are increased due to increase of capacitance values for graphite electrodes modified by

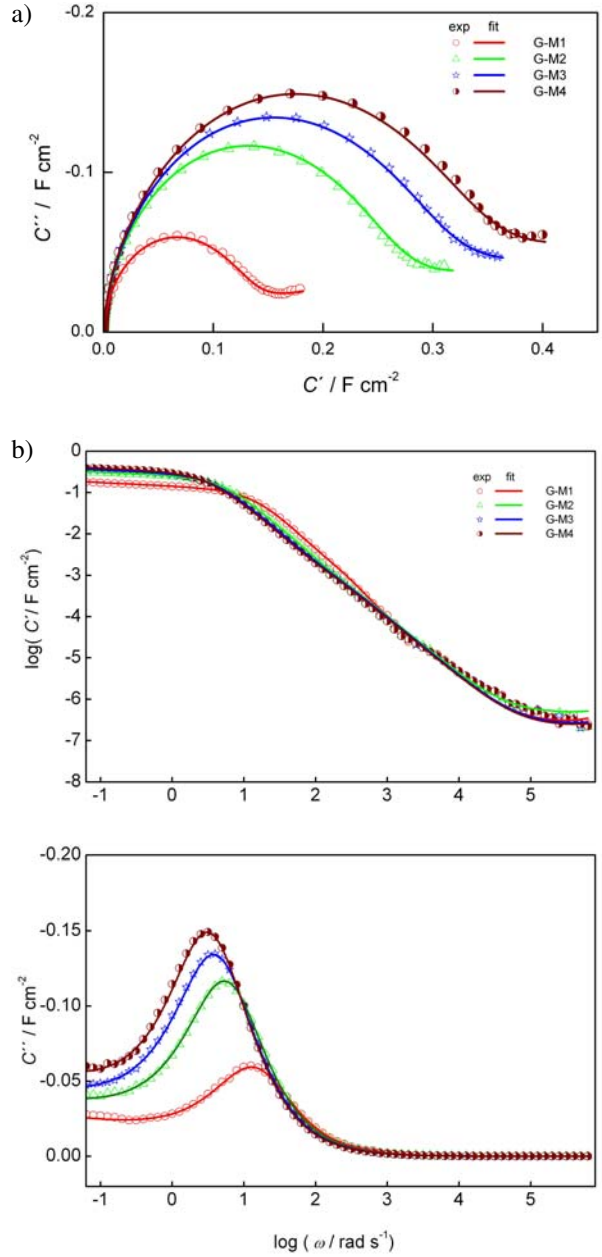

Fig. 5. (a) Complex capacitance dispersion (*C´´ vs. C´*) and (b) log *C´* and *C´´ vs.* log ω of electrochemically modified graphite electrodes in 0. 5 mol dm^{-3} H_2SO_4, measured at –0.20 V *vs*. MSE.

higher number of cycles. Fig. 5b shows real, *C´* and imaginary parts, *C´´*, as functions of ω. For all presented electrodes, log *C´* values increase with decrease of frequency up to the constant values, determining low frequency capacitance values, whereas *C´´* values formed peak-curved lines from which the characteristic frequency, determining the rate of charging/discharging of the overall capacitance can be evaluated.

Influence of potential change on impedance spectra of modified graphite electrodes are in the form of Bode plots shown in Figure 6, where impedance spectra of mo-

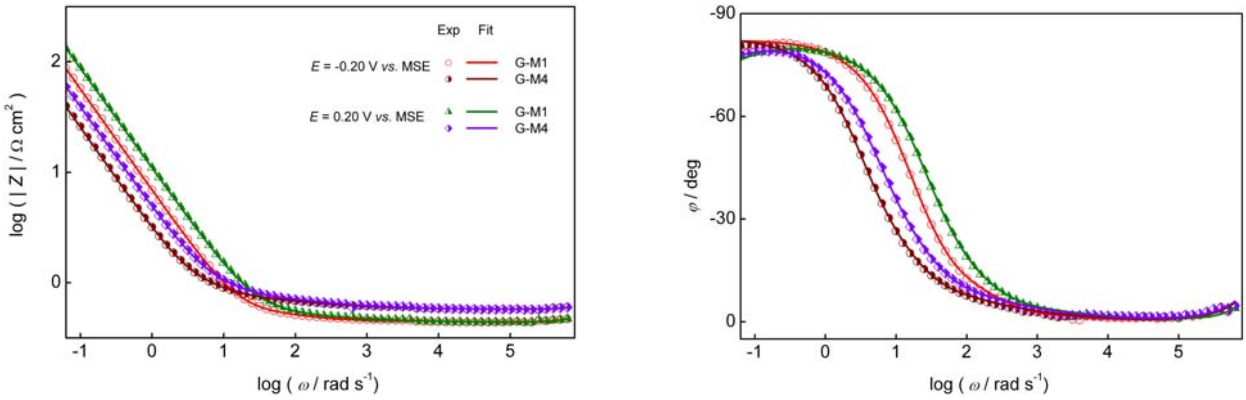

Fig. 6. Bode plots (log| *Z*| and φ *vs.* log ω) of electrochemically modified, GM-1 and GM-4 graphite electrodes in 0.5 mol dm^{-3} H_2SO_4 measured at –0.20 and 0.20 V *vs*. MSE

dified GM-1 and G-M4 graphite electrodes measured at different potential values can be compared.

According to Fig. 6, there are not many changes in the overall resistive/capacitive shapes of impedance spectra measured at two different potential values, except that higher capacitive impedance(s) are measured at higher potential value(s). Also, certain decrease of $-\varphi$ values at few points of the lowest frequencies can be observed for both modified graphite electrodes at 0.20 V *vs*. MSE. Similar differences between impedance spectra measured at –0.20 and 0.20 *vs*. MSE were obtained for other modified graphite electrodes too.

3. 3. Impedance Modeling of Graphite Electrodes

In real experimental conditions of three-electrode cell, the measured electrode impedance, $Z_{el}(i\omega)$, consists of interfacial, Z_{in} $(i\omega)$, and not interfacial parts, according to:[20,31]

$$Z_{el}(i\omega) = R_{HF} + Z_{in}(i\omega) \quad (3)$$

R_{HF} in eqn. (3) is the sum of resistive contributions including solution resistance of the layer formed between the surface of working and reference electrode, resistance of the working electrode, contact resistance between particles and support, etc.[20] Here, contributions of experimental artefacts to high frequency data, caused by measurements of low impedances in a three-electrode cell[31] must also be taken into account. The way of evaluation of the corresponding artefact impedance parameters, L^* and C^* has been described previously.[32]

For weakly distributed capacitive impedance spectra, the interfacial impedance, $Z_{in}(i\omega)$, has usually been described using the constant phase element, CPE, model. CPE is the most commonly applied model for capacitive dispersions and related mostly to locally distributed electrode surface irregularities of various origins.[20–22] Frequency dependence of interfacial impedance showing CPE type of impedance response is defined as:

$$Z_{in}(i\omega)_{CPE} = [Q\,(i\omega)^{\alpha}]^{-1} \quad (4a)$$

$$Y_{in}(i\omega)_{CPE}(i\omega)^{-1} = Q\,(i\omega)^{\alpha-1} \quad (4b)$$

Eqn. (4) defines the CPE impedance in terms of two frequency independent parameters Q and α, where for $\alpha = 1$, Q in $\Omega^{-1}s^{\alpha}$, becomes a pure capacitance, C in F. Simulations drawn in Figure 7 anticipate the expected shapes of a capacitive electrode impedance in Nyquist and Bode plots, in dependence of α. Calculations are made using eqns. (2) and (4) for given values of R_{HF}, Q and α.

Fig. 7 shows that eqn. (4) predicts an inclined capacitive line with α dependent and constant slope at all frequencies of Nyquist plots, as well as α dependent width of transition frequencies in Bode phase plots, respectively. These shapes in Fig. 7 are, however, different from those observed in Figs. 3b, 4 and 6, where different slopes at different frequencies and lengthy transition frequency ranges can clearly be observed. Highly distributed capacitance effects as observed in Fig. 3b for all modified graphite electrodes at higher frequencies, can generally be accounted for by applying the concept of cylindrical porous electrodes.[26] In the simplified form, impedance/frequency function of a porous electrode can be described by the *so called* transmission line element, TL,[19] with frequency dependence of impedance defined as:[29,30]

$$Z_{in}(i\omega)_{TL} = R_w(i\omega\tau)^{-1/2}\coth(i\omega\tau)^{1/2} \quad (5a)$$

$$\tau = R_w C_w = L^2/D \quad (5b)$$

Eqn. (5) models the interfacial capacitance of pore walls in conditions of highly conductive material having uniform porosity, where porosity is defined by radius and number of pores.[29] R_w, τ, C_w and D in eqn. (5) are porosity dependent solution resistance due to ion transport within

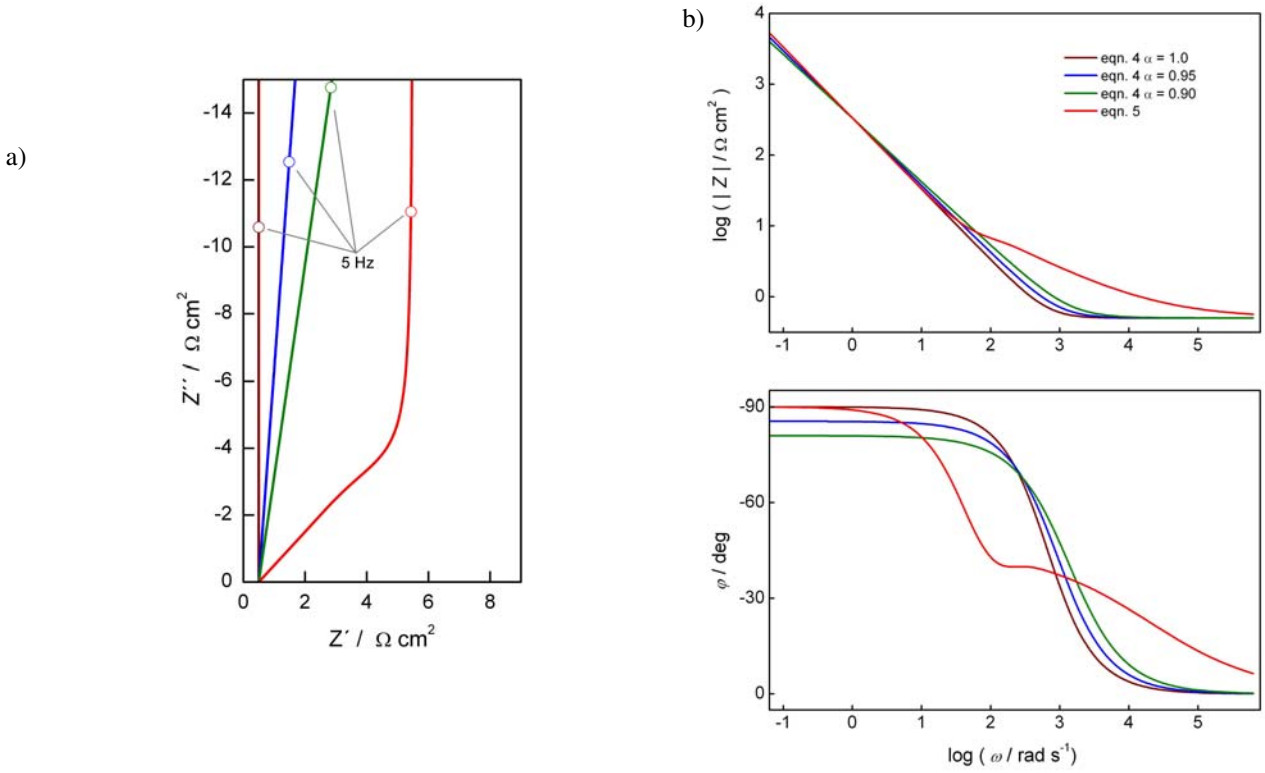

Fig. 7. Simulations of (a) Nyquist (Z'' *vs.* Z') and (b) Bode ($\log|Z|$ and φ *vs.* $\log \omega$) plots calculated by eqn. (3), $R_{HF} = 0.5\ \Omega\ cm^2$ and: eqn. (4), $Q = 0.003\ \Omega^{-1}\ cm^{-2}\ s^{\alpha}$ and denoted α; eqn. (5), $R_w = 15\ \Omega\ cm^2$, $\tau = 0.045$ s.

the pores, characteristic relaxation time due to finite length, L, of the pores, total capacitance of pore walls and diffusion coefficient of electrolyte ions inside the pores, respectively. Simulated impedance spectrum calculated using eqn. (3) in combination with eqn. (5) for C_w values similar to Q already used in impedance simulations, is also drawn in Fig. 7, showing significant differences in higher frequency parts of Nyquist plots and phase Bode plots, respectively. Frequency dependences of experimentally measured impedance spectra presented in Figs. 3, 4 and 6, and these simulated using either eqn. (4) or eqn. (5) and presented in Fig. 7, are not the same and so would hardly give good fitting results. This is supported by data in Table 1, showing in the first two rows impedance parameter values and poor fitting results obtained by using of eqn. (3) combined with either eqn. (4) or eqn. (5) and experimental data of modified, GM-4, graphite electrode presented in Figs. 3–5. Note that in all Tables presented in this paper, the minimal number of significant digits with respect to standard deviations is reported for each impedance parameter value, whereas S denotes the weighted sum of errors for the overall fits defined by eqn. (1).

The phenomenon of obtaining poor fits by using eqn. (5) in representation of porous and/or intercalation systems, points immediately toward pore or particle size distributions.[34,35] It has already been shown that fittings based on n parallel diffusion paths defined by eqn. (5), describing different electrode segments, can significantly improve results.[34,35] When in addition, the exponents are not fixed strictly to ½ and defined as $p \leq 0.5$, the following

Table 1. Values of impedance parameters of G-M4 graphite electrode in 0.5 mol dm^{-3} H_2SO_4, calculated by CNLS fittings of denoted equations to corresponding impedance spectra in Figs. 3–5.

Graphite	Eqns.	R_{HF}/ Ω cm²	R_{W1}/ Ω cm²	τ_1/ s	p_1	Q_1/ $\Omega^{-1}\ s^{\alpha}\ cm^{-2}$ (α)	R_{W2} / Ω cm²	τ_2/ s	p_2	S
G-M4	(3)+(4)	0.622	–	–	–	0.32×10^{-2} (0.866)	–	–	–	5.46
	(3)+(5)	0.566	0.56	0.157	0.457	–	–	–	–	0.16
	(3)+(6)	0.570	0.58	0.085	0.46	–	2.6	0.38	0.47	0.047

C^*/ F cm^{-2} = 2.9 – 9.3 × 10^7 ; L^*/ H cm^2 = 2.1 – 2.2 × 10^{-7} fitted after[32]

equation for capacitive interfacial electrode impedance of a porous electrode, showing different diffusion paths, can be defined as:

$$Z_{in}(i\omega)_{\sum TL} = (\sum_1^n (R_{wn}(i\omega\tau_n)^{-p} \coth(i\omega\tau_n)^p)^{-1})^{-1} \quad (6)$$

Efficiency of two diffusion paths model described by eqn. (6) $n = 2$, is supported by data listed in the last row of Table 1, showing significantly improved statistics in the case of fitting of eqn. (6) to impedance spectra of G-M4 graphite electrode. Although having generally low relaxation times, due to $\tau_1 \neq \tau_2$, two TLs of G-M4 graphite are both visible and resolvable, what makes the statistic of fittings much better.

To account for bending of phase angles such as these observed at few lowest frequencies for G-M1 graphite measured at –0.20 V and all modified graphite electrodes measured at 0.20 V *vs*. MSE, the low frequency resistance, R_p is introduced in the fitting procedure, by defining $Z(i\omega)_{in}$ from eqn. (3) as:

$$Z_{in}(i\omega) = ((Z_{in}(i\omega))_{\sum TL})^{-1} + R_p^{-1} \quad (7)$$

Inclusion of some high valued R_p for accounting possible side and insubstantial reactions is the usual procedure in fittings of otherwise capacitive systems[16]. Here, the fitted results obtained using eqn. (3) in combination with eqn. (7) $n = 2$, are for all modified, G-M1 to G-M4, graphite electrodes drawn by full lines in Figs. 3–6 and collected in Table 2, together with total capacitance, ($C_{W1} + C_{W2}$) values, roughly calculated using R_W and τ values and eqn. (5b). Note that in the fitting procedure, R_p is considered as the contributing parameter whenever its presence decreased *S* value considerably and its standard deviation is lower than 30%. In all other cases, R_p is omitted from eqn. (7), what is denoted by tittles in the R_p related column of Table 2.

The main points appearing from Table 2 can be summarized as acceptable fitting results indicating that all modified graphite electrodes are porous with some pore size disribution. Pore structure is obviously changed by number of potential cycles applied during modification, what is seen through continuous increase of all pore structure related values (τ_1, τ_2, R_{W1} and R_{W2}). The overall capacitances induced at pore walls, expressed in Table 2 as ($C_{W1} + C_{W2}$) values are in reasonable agreement with capacitance values in Fig. 1b at –0.20 V and 0.20 V *vs*. MSE. As in Fig. 1b, increase of capacitance values with increased number of potential cycles should be related to increased surface area and higher content of residues of oxygen containing surface groups, formed initially by oxidation at anodic potentials during modification. By higher content of oxygen containing groups, higher pseudocapacitance will be induced, contributing more to the overall capacitance values, particularly near peak potential value(s) of their redox reaction (*cf.* Fig. 1b). According to Table 2, lower capacitance values obtained for modified graphite electrodes measured at higher potential value, should primarily be related to decrease of τ_1 and τ_2 values. As in the case of porous GC electrode,[29] such decrease suggests increase of diffusion coefficient, D, value (*cf.* eqn. 5b), *i.e.* potential changes of solution properties within the pores. Different redox forms of oxygen containing groups at –0.20 and 0.20 V *vs*. MSE and also increased extent of intercalation of HSO_4^- ions at higher anodic potentials, could form a basis for changes of D values. Continuous increase of R_{HF} values for graphite electrodes modified with higher number of potential cycles indicates possible increase of graphite electrode resistivity, and/or some kind of electrode surface blockage. Both effects could be related to increased amounts of graphite oxide residues, remaining at the graphite surface after reduction process.

4. Conclusions

In this work, graphite electrodes, modified by potential cycling between potentials of oxide film formation and reduction in the sulphuric acid, have been characterized by EIS. Impedance spectra measured at two different potential values within double-layer region of graphite are

Table 2. Values of impedance parameters of electrochemically modified G-M1 to G-M4 graphite electrodes in 0.5 mol dm^{-3} H_2SO_4, calculated by CNLS fittings of eqns. (3) and (7) $n = 2$ to the corresponding impedance spectra in Figs. 3–6.

Graphite	E / V *vs.* MSE	R_{HF} / Ω cm^2	R_{W1} / Ω cm^2	τ_1 / s	p_1	R_{W2} / Ω cm^2	τ_2 / s	p_2	R_p / Ω cm^2	($C_{W1} + C_{W2}$) / F cm^2
G-M1	–0.20	0.434	0.16	0.008	0.47	0.8	0.05	0.46	1473	0.111
	0.20	0.431	0.18	0.005	0.46	0.8	0.03	0.46	1500	0.062
G-M2	–0.20	0.488	0.34	0.028	0.45	1.0	0.14	0.47	–	0.216
G-M3	0.20	0.541	0.56	0.056	0.46	1.4	0.24	0.47	–	0.263
G-M4	–0.20	0.570	0.58	0.085	0.46	2.6	0.38	0.47	–	0.292
	0.20	0.570	0.56	0.047	0.46	2.6	0.23	0.46	856	0.174

C^*/ F cm^{-2} = 0.87 – 1.00 × 10^6, L^*/ H cm^2 = 2.0 – 2.1 × 10^7 fitted after[32] S = 0.015 – 0.047

compared for various extents of graphite modification, attained by different number of potential cycles applied.

Similarly layered structures of expanded graphite evident by SEM imaging of all modified graphite electrodes are accompanied by almost capacitive impedance spectra responses, showing decreased impedance magnitudes with either increased number of potential cycles or lowering of potential values. This can be related to increased surface area and higher pseudocapacitive contributions of residues of oxygenated surface groups formed by initial oxidation steps.

Some peculiar features of higher frequency parts of impedance spectra, indicating high extent of capacitive distributions, precluded impedance modeling of graphite in usual terms for accounting surface irregularities or uniform porosity effects. Good matching between experimentally measured data and data calculated on the basis of two finite diffusion paths impedance model, supported by statistical results, suggests formation of porous graphite surface containing two classes of pores.

The evaluated impedance parameter values show continuous changes with stages of graphite modification, indicating continuous structural changes of pores by increased number of potential cycles applied. Differences of impedance parameter values at two potential values suggest some changes in solution properties within the pores, what can be connected with different redox forms of oxygenated surface groups and/or higher extent of possibly intercalated HSO_4^- ions.

A clear tendency of graphite surface damaging for the highest number of potential cycles applied, indicates possible effects of graphite surface corrosion, sulfuric acid penetration during longer time spent at the highest anodic potentials, and disorderd stacking of expanded graphite.

5. Acknowledgements

This work is supported by the MSES, Croatia, under project 098-0982904-2905.

The authors acknowledge to Marijan Marciuš from the Rudjer Bošković Institute for SEM imaging.

6. References

1. R. L. McCreery, *Chem. Rev*. **2008**, *108*, 2646–2687.
2. B. E. Conway, Electrochemical Supercapacitors: Scientific fundamentals and technological applications, Kluwer Acad./Plenum Pub. New York. **1999**, pp. 183–257.
3. F. Kang, T.-Y. Zhang, Y. Leng, *Carbon*, **1997,** *35,* 1167–1173.
4. D. Alliata, R. Kötz, O. Haas, H. Siegenthaler, *Langmuir*, **1999,** *15*, 8483–8489.
5. Y.-R. Shin, S.-M. Jung, I.-Y. Jeon, J.-B. Baek, *Carbon*, **2013,** *52*, 493–498.
6. H. Xu, X. Fan, Y. Lu, L. Zhang, X. Kong, J. Wang, *Carbon,* **2010,** *48*, 3300–3303.
7. K. H. Jeong, S. M. Jeong, *Electrochim. Acta,* **2013,** *108*, 801–807.
8. S. Stankovich, D. A. Dikin, R. D. Piner, K.A. Kohlhaas, A. Kleinhammes, Y. Jia, J. Wu, S. T. Nguyen, R. S. Ruoff, *Carbon,* **2007,** *45*, 1558–1565.
9. Y. Geng, Q. Zheng, J.-K. Kim, J. Nanosci. *Nanotechnol.* **2010,** *10*, 1–8.
10. Y. Hong, Z. Wang, X. Jin, *Scientific Reports*, **2013,** 3:3439.
11. M. D. Stoller, S. Park, Y. Zhu, J. An, R. S. Ruoff, *Nano Letters,* **2008,** *8*, 3498–3502.
12. S. Guo, S. Dong*, Chem. Soc. Rev.* **2011,** *40*, 2644–2672.
13. J. Navarro-Laboulais, J. Trijueque, J. J. Garcia-Jareño, D. Benito, F. Vicente, *J. Electroanal. Chem.* **1998,** *444*, 173– 186.
14. M. D. Levi, E. Levi, Y. Gofer, D. Aurbach*, J. Phys. Chem.* B, **1999,** *103*, 1499–1508.
15. M. Holzapfel, A. Martinent, F. Alloin, B. Le Gorrec, R. Yazami, C. Montella*, J. Electroanal. Chem.* **2003**, *546*, 41–50.
16. F. La Mantia, J. Vetter, P. Novak, *Electrochim. Acta,* **2008**, *53*, 4109–4121.
17. A. Casero, A. M. Parra-Alfambra, M. D. Petit-Domínguez, F. Pariente, E. Lorenzo, C. Alonso, *Electrochem. Commun.* **2012**, *20*, 63–66.
18. A. Bonanni, M. Pumera, Electrochem. Commun. **2013**, *26*, 52–54.
19. J. R. Macdonald, (Ed.), Impedance Spectroscopy, Emphasizing solid materials and systems, J. Wiley & Sons, New York, **1987**.
20. M. E. Orazem, B. Tribollet, Electrochemical Impedance Spectroscopy, J. Wiley & Sons, Hoboken, New Jersey, **2008**.
21. B. Emmanuel, *J. Electroanal. Chem.* **2007**, *605*, 89–97.
22. T. Pajkossy, D. M. Kolb*, Electrochim. Acta*, 2**008**, *53*, 7403–7409.
23. M. S. Yazici, D. Krassowski, J. Prakash*, J. Power Sci.* **2005**, *141*, 171–176.
24. W. J. Basirun, M. Sookhakian, S. Baradaran, M. R. Mahmoudian, M. Ebadi, *Nanoscale Res. Lett.* **2013**, 8:397.
25. V. I. Vigdorovich, L. E. Tsygankova, V. I. Kichigin, I. E. Gladysheva, *Protect. Met. Phys. Chem. Surf.* **2012**, *48*, 438–443.
26. R. De Levie, in: P. Delahay, Ed., Advances in Electrochemistry and Electrochemical Engineering, Vol. VI, Interscience, New York, **1967**. p. 329.
27. K. Honda, T. N. Rao, D.A. Tryk, A. Fujishima, M. Watanabe*, J. Electrochem. Soc*. **2001**, *148*, A668–A679.
28. Y.-R. Nian, H. Teng, *J. Electroanal. Chem.* **2003**, *540*, 119–127.
29. M. G. Sullivan, R. Kötz O. Haas, *J. Electrochem. Soc.* **2000**, *147*, 308–317.
30. K. Magdić, K. Kvastek, V. Horvat-Radošević*, Electrochim. Acta,* **2014**, *117*, 310–321.
31. S. Fletcher, *Electrochem. Commun.* **2001**, *3*, 692–696.
32. V. Horvat-Radošević, K. Kvastek, *J. Electroanal. Chem.* **2009**, *631*, 10–21.
33. H. Liu, C. Yan, Y. Qiao*, Electrochim. Acta,* **2011**, *56*, 8783–8790.

34. M. D. Levi, C. Wang, D. Aurbach, *J. Electroanal. Chem.* **2004**, *561*, 1–11.

35. M. Itagaki, S. Suzuki, I. Shitanda, K. Watanabe, H. Nakazawa, *J. Power Sourc.* **2007**, *164*, 415–424.

Povzetek

Elektrokemijsko impedančno spektroskopijo, EIS, smo uporabili za karakterizacijo elektrokemijsko modificiranih grafitnih elektrod v raztopini žveplove kisline. Modifikacijo grafita smo izvedli s cikliranjem potenciala med vrednostima za reakcijo oksidacije oziroma redukcije grafitnega oksida. Na lastnosti modificiranega oksida smo vplivali z izborom števila ciklov ter z dolžino časovnega intervala, znotraj katerega je potekala redukcija po končanem cikliranju. Impedančne spektre, ki smo jih izmerili pri dveh potencialih znotraj območja električne dvoplasti na grafitu, smo opisali z ustreznim modelom. Uporabili smo koncept porozne elektrode z dvema difuzijskema potema za elektrolit, s čimer smo predpostavili obstoj dveh vrst por. Izračunani impedančni parametri kažejo zvezno spreminjanje vrednosti glede na stopnjo modifikacije grafita, kar kaže na zvezno spreminjanje strukture por s številom ciklov. Razlike v vrednostih impedančnih parametrov pri dveh različnih vrednostih potencialov kažejo na spremembe v lastnostih raztopine, ki jih v porah modificiranega grafita povzroči vsiljeni potencial.